

MULTI OBJECTIVE OPTIMIZATION OF LAMINAR MIXED CONVECTIVE HEAT TRANSFER OF ELECTRONIC CHIPS IN A HORIZONTAL CHANNEL WITH VORTEX GENERATOR

S K MANDAL¹, DIPAK SEN², & ASIS GIRI³

^{1,2}Department of Mechanical Engineering, National Institute of Technology, Arunachal Pradesh, India.

³Department of Mechanical Engineering, North Eastern Regional Institute of
Science and Technology, Arunachal Pradesh, India

ABSTRACT

This paper represents laminar mixed convective heat transfer in a channel (horizontal) including five electronic chips mounted on the bottom wall with a vortex generator (triangular bar), VG and is carried out in order to maximize heat transfer rate numerically. The effect of position of vortex in horizontal and vertical distance (0.3 - 0.4) of VG on heat transfer has been investigated thoroughly to observe the dependence of heat transfer on both. The finite volume method and the SIMPLE algorithm are used to solve the conservation equations of mass, momentum, and energy for mixed convection. The Reynolds number changes from 50 to 250. Numerical simulations demonstrate inclusion of vortex generator and results in the substantial enhancement in heat transfer in terms of Nusselt number, Nu, as compared to without vortex generator. The results obtained also show that the Reynolds number and the position of vortex in horizontal and vertical have considerable effects on the improvement of the heat transfer inside the channel. Box Behnken design was used to study the interaction between the parameters which influences the Nusselt number. Highest Nusselt number 16.08 was observed for x/H , y/H and Re at 8.5, 0.4 and 250 respectively. A significant interaction was observed between x/H , h/H with Re .

KEYWORDS: Mixed Convection, Horizontal Channel, Vortex Generator & RSM

Received: Nov 18, 2017; **Accepted:** Dec 08, 2017; **Published:** Dec 30, 2017; **Paper Id.:** IJMPERDFEB201818

I. INTRODUCTION

Electronics equipment and devices currently play a major part in almost all sphere of our day-to-day life starting from electronic toys, high-power computer appliances, mobile, space craft, control of power plant, etc. to mention a few. Electronic equipment under perform if it crosses the specified temperature limit. To augment the reliability and life anticipation of an electronic device, the cooling of electronic equipment is one of the main barriers as it was inversely related to the temperature of electronic components [1].

Since the publication of the classic papers of Graetzin 1883 on forced convection, Elenba as in 1942 on natural convection and Ostrach in 1954 on mixed convection, the subject of channel convection received much attention as revealed by the excellent reviews of Shah and London in 1978, Ostrach in 1964, Raithby and Hollands in 1985 and Aung in 1987 [2-10]. Studies of heat transfer enhancement on blocked channel flows point toward that most of the studies are paying attention on forced convection with support of vortex generator with different shape. Wu and Perng studied the heat transfer enhancement by placing an oblique plate for internal flow

adjustment induced by vortex shedding [11]. Their results show that due to inclusion of an oblique plate in cross flow above an upstream block can effectively increase the heat transfer performance of mixed convection in the channel, whereas Valencia [12] used rectangular bar for the improvement of same. An inclined block shape vortex generator was used by Sohankar and Davidson [13] in their investigation. This investigation performed in case of three dimensional unsteady flows where Reynolds number 400-1500. An oscillating rectangular bar is used by Yang [14] to improve heat transfer of electronic equipment. The oscillating bar took active participation in vortices generation. He adopted Galerkin finite element method to solve the flow equations. In 2002, Wang and Jaluria [15] examined the effect of a vortex promoter placed between the horizontal walls of a channel on the mixed convection heat transfer of two downstream protruding isothermal blocks using a two-dimensional model and report enhanced heat transfer due to resonant effect. Alahyari Beig et.al [16] investigates the optimal position of a triangular bar which act as a vortex generator in a blocked channel for heat transfer enhancement of electronic chips. Body force and viscous dissipation was ignored. Genetic algorithm combined with Gaussian process was used as the optimization algorithm. The use of multivariate quadratic equation based optimization has been explored using Response Surface Methodology (RSM). In RSM, comparative precise prediction of input-output relationships can be established [17]. One of the advantages of using RSM over other conventional experimental methods are reduction of the experimental cost and minimizing the variability around the target value. Another advantage is that optimal working conditions, determined from the simulation or laboratory study, can be reproduced in real applications [20] It has been vastly applied in several fields of Thermal and Manufacturing for the purpose of optimization [18-20].

In the present study, the mixed convection is used for cooling five electronic chips mounted in a rectangular horizontal channel. Our objective is to study electronic chip cooling placed in a triangular block that acts as a vortex generator in front of chip and thereby deciphering its positional effect on the chip cooling. Investigation of mutual interaction between the parameter which might influence the heat transfer via convection viz. Reynolds number and position of vortex generator was studied using Box-Behnken design. From the response surface methodology, optimum combinations of the parameters were predicted to maximize heat transfer in the channel.

2. PROBLEM DESCRIPTION

A schematic of a horizontal channel with five numbers of identical Electronic chips and an adiabatic triangular cross-sectional block which will be acting as a vortex generator is shown in Figure 1. The dimensions are normalized using the channel height H . The fluid enters the channel with a uniform velocity and temperature. The fluid is colder than the Chips with the inlet temperature of 20°C and the heat generated by each Chip is equal to 1000 W/m^2 . The thermal properties of the air are assumed to be constant and the buoyancy effects are also considered. Distance from inlet to first chip L_1 , each chip width w , distance between two neighbouring chip d , height of chip h , distance from channel outlet to last chip L_2 . Channel length is L . Vortex dimension and position also shown.

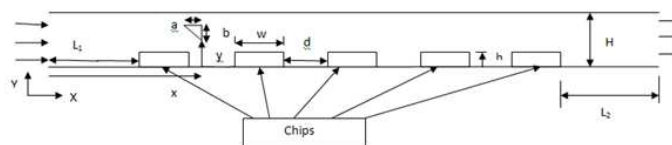


Figure 1

2.1. Governing Equations

The continuity, momentum and energy equations for steady two-dimensional laminar incompressible Newtonian fluid are considered. Using non-dimensional variables, the non-dimensional governing equations are obtained as

Continuity

$$\frac{\partial U}{\partial X} + \frac{\partial V}{\partial Y} = 0 \quad (1)$$

X-momentum

$$\frac{\partial U}{\partial X} + U \frac{\partial U}{\partial X} + V \frac{\partial U}{\partial Y} = -\frac{\partial P}{\partial X} + \frac{1}{Re} \left(\frac{\partial^2 U}{\partial X^2} + \frac{\partial^2 U}{\partial Y^2} \right) \quad (2)$$

Y-Momentum

$$\frac{\partial V}{\partial Y} + U \frac{\partial V}{\partial X} + V \frac{\partial V}{\partial Y} = -\frac{\partial P}{\partial Y} + \frac{1}{Re} \left(\frac{\partial^2 V}{\partial X^2} + \frac{\partial^2 V}{\partial Y^2} \right) + \frac{Gr}{Re^2} \theta \quad (3)$$

Energy

$$\frac{\partial \theta}{\partial X} + U \frac{\partial \theta}{\partial X} + V \frac{\partial \theta}{\partial Y} = \frac{1}{RePr} \left(\frac{\partial^2 \theta}{\partial X^2} + \frac{\partial^2 \theta}{\partial Y^2} \right) \quad (4)$$

Appearing in Eqs. (2), (3) and (4) Pr, Re and Gr are the Prandtl, Reynolds and Grashop numbers, respectively, which are defined as

$$Pr = \frac{\nu}{\alpha}, \quad Re = \frac{\rho v D_h}{\mu}, \quad Gr = \frac{g \beta T D_h^3}{\nu^2} \quad (5)$$

where β and ν are the thermal expansion coefficient and the kinematic viscosity of the fluid, respectively.

The non-dimensional parameters are listed as

$$X = \frac{x}{H}, \quad Y = \frac{y}{H}, \quad U = \frac{u}{u_{in}}, \quad V = \frac{v}{u_{in}}, \quad P = \frac{p}{\rho u_{in}^2}, \quad \theta = \frac{T - T_{in}}{T_s - T_{in}} \quad (6)$$

The heat transfer is measured by local Nusselt number which can be written as

$$Nu_x = \frac{h_x D}{k} \quad (7)$$

The average Nusselt number can be calculated by

$$Nu = \frac{1}{L} \int Nu_x \, dx \quad (8)$$

2.2 Boundary Condition

Boundary condition of the problem as follows:

At the inlet of the channel

$$u = u_{inlet}, \quad T = T_{atm} \quad (9)$$

In Eq. 5 u_{inlet} varies with varying Reynolds number as per the cases.

At the outlet of the channel

$$P = P_{atm}, \quad \frac{\partial T}{\partial \eta} = 0 \quad (10)$$

All wall surfaces and vortex surface

$$u = v = 0, \quad T = T_{wall} \quad (11)$$

All chip surfaces

$$-k \frac{\partial T}{\partial \eta} = q'' \quad (12)$$

3. NUMERICAL APPROACH

Assumptions like steady two-dimensional laminar incompressible flow with constant air properties (at 293 K) has been made to have numerical model of fluid flow and heat transfer. The finite volume method and the SIMPLE algorithm are used to solve the governing equations (Eq. 1-4) subjected to boundary conditions (Eq. 9-12) for mixed convection. Ansys 16.2 software was used for the simulation. Discretization of energy and momentum equations is performed by 2nd order upwind scheme. The convergence criteria are considered as in order of 10^{-3} for continuity, x-velocity and y-velocity and for energy 10^{-6} . The obtained simulation data was processed using statistical software package MiniTab version 15.10, MiniTab Inc, Pennsylvania, USA to analyze the simulation design.

4. MULTI PARAMETER OPTIMIZATION

The cumulative effect of two process parameter viz. Vortex position and Reynolds number was studied by multi parameter optimization. The variables so chosen were vortex position (x/H, y/H) and Reynolds number (Re). Response variable measured was cumulative average Nusselts number. A three factor Box-Behnken design with 15 unique sets and a triplicate on the centre point was used and coded [21]. The independent variables were coded according to Eq. 13

$$x_i = \frac{X_i - X_{i, mid}}{\Delta X_i} \quad (13)$$

Where the ith independent variable is represented by x_i . The uncoded value of the ith independent variable and the uncoded value at the centre point for the ith independent variable are represented by $X_i, X_{i, mid}$, respectively. The x/H varies from 4.5 to 12.5 in steps of 2, y/H varies from 0.3 to 0.4 in steps of 0.05, Reynolds number varies from 50 to 250 in steps of 50 and average Nusselts number was calculated. Development of Regression Equation was done using statistical software, Minitab 15. A second degree polynomial Eq. 14 was used to fit the simulation data.

$$Y = C_1 + C_2 X_1 + C_3 X_2 + C_4 X_3 + C_5 X_1^2 + C_6 X_2^2 + C_7 X_3^2 + C_8 X_1 X_2 + C_9 X_2 X_1 + C_{10} X_2 X_3 \quad (14)$$

The multivariate equation Eq.14 Can be concurrently solved by analyzing response surface methodology. It helps in visualising the individual and collective effect of the independent variables on the dependent variable. It also determines the mutual interactions between the independent variables and their subsequent effect on the dependent variable.

5. GRID INDEPENDENCY AND VALIDATION

5.1. Grid Independency Test

In order to achieve grid independent solutions, a grid independence test was conceded for four different nodes. A non-uniform grid was used for all over the domain. Very fine grids are used in front of the chips and vortex.

Table No: 1

SL No	Node/Element	Temperature (K) at Chip1	% of Change	Nu at Chip 1	% of Change
1	18592/17097	391.09	-----	11.54	-----
2	57363/54436	388.17	0.75%	11.70	1.39%
3	84978/81269	386.36	0.47%	12.05	2.99%
4	97220/93193	384.69	0.43%	12.17	0.99%

Result of the grid independence study for $Re=50$, heat flux= 1000w/m^2 , $x/H=4.5$, $y/H=0.3$ are given in table no. 1 for temperature and Nu at Chip1. When the number of nodes increased from 84978 to 97220 for computation, a change of only 0.99% was observed on the surface Nusselt number and a change of only 0.43% was observed on temperature at chip 1. Hence a node of 84978 is found to meet the requirements for computational time limits.

5.2. Validation

Present work validated with the work of Alahyari Beig et.al [16] maintaining same test domain and parameter used by them. The difference in result of present work and the work of Alahyari Beig et.al lies between 2%, shown in table no. 2. It indicates that the results show good agreement with the literature data.

Table No: 2

Position of Vortex		Temperature as Per the Work of Alahyari Beig et.al at $Re=400$			Temperature as Per the Present Work at $Re=400$		
X-position	Y-position	T ₁ (K)	T ₂ (K)	T ₃ (K)	T ₁ (K)	T ₂ (K)	T ₃ (K)
5.286	0.620	332.8	352.7	360.9	330.65	349.83	357.51
9.288	0.594	343.6	346.1	355.2	341.18	344.76	354.90
9.413	0.580	343.6	347.0	354.4	341.24	340.99	354.31

6. RESULTS AND DISCUSSIONS

The numerical study has been conducted on two-dimensional, steady state, laminar mixed convection in a rectangular horizontal channel after introducing an adiabatic triangular bar. Body force and viscous dissipation also considered. Present investigation has been conducted for diverse Reynolds number ($Re= 50, 100, 150, 200, 250$) and different location of vortex generator ($x/H= 4.5, 6.5, 8.5, 10.5, 12.5$ and $y/H= 0.3, 0.35, 0.4$) to generate sufficient data of local Nusselt number (Nux) and Average local Nusselt number (Nu_{avg}). Air was used as cooling medium as it was used in most of the practical cases in electronic system. Ambient temperature was considered 293 K. All results were presented in dimensionless values. In this present study dimensions are taken to be $L_1=5H$, $L_2=5H$, $d=w$, $w/H=2$, $h/H=0.25$ and triangular bar dimensions $a/H=1/8$, $b/H=1/4$. Present investigation has two stage of numerical study. Firstly investigation was done without using the triangular bar which acts as a vortex generator within the channel. After that considering a triangular bar at different location within the channel.

6.1. Effect of Insert of Vortex

Using streamline the flow field structure is characterized, with uniform profile of temperature and uniform velocity the fluid thrust into the channel. Streamline and temperature contour at $Re=150$ are portrayed in Figure 2(a-b) in case of without vortex. In Figure 3(a-c) streamlines are portrayed at $Re=150$ at different vortex location within the channel, and in Figure 4(a-c) are temperature contour for the same.

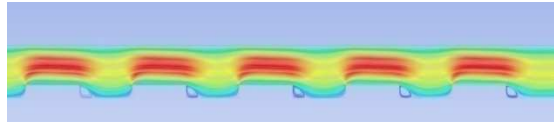


Figure 2(a): Streamline at $Re=150$, with out Vortex

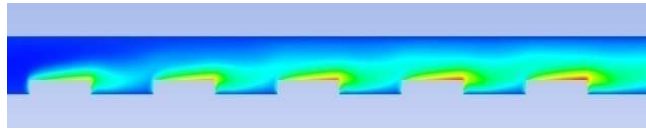


Figure 2(b): Temperature Contour at $Re=150$, with out vortex

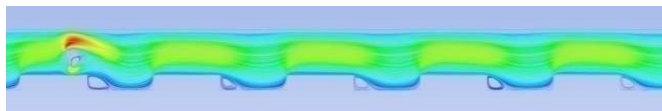


Figure 3(a): Streamline at $Re=150$, with Vortex Position $x/H=6.5$, $y/H=0.4$

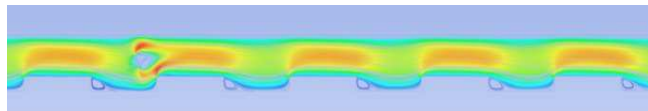


Figure 3(b): Streamline at $Re=150$, with Vortex Position $x/H=8.5$, $y/H=0.4$

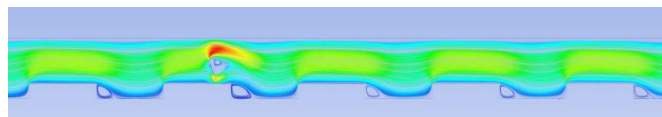


Figure 3(c): Streamline at $Re=150$, with Vortex Position $x/H=10.5$, $y/H=0.4$

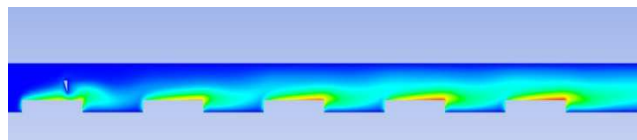


Figure 4(a): Temperature Contour at $Re=150$, with Vortex Position $x/H=6.5$, $y/H=0.4$

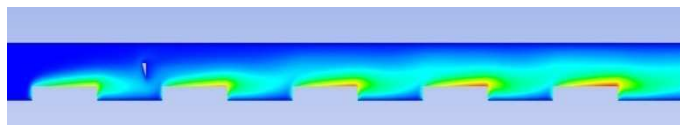


Figure 4(b): Temperature Contour at $Re=150$, with Vortex Position $x/H=8.5$, $y/H=0.4$

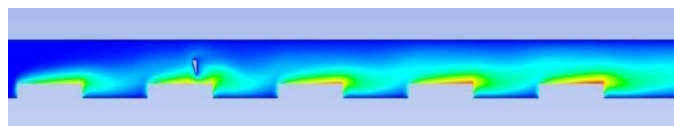


Figure 4(c): Temperature Contour at $Re=150$, with Vortex Position $x/H=10.5$, $y/H=0.4$

All Figures shown above (Figure 2-4) are just a portion of whole channel. Temperature rise at chip 1 is much lesser than other chips as because chip 1 exposed to cooler air than other ones. In Figure 2(II) also shows that thermal boundary layer much thinner at the top of first chip compared to other chips. In case of the channel with triangular bar, not only at chip 1, but also in other position of the channel thermal boundary layer much thinner as shown in Figure 4(a-c), which signifies enhancement of heat transfer after the inclusion of triangular bar within the channel. Figure 3(a-c)

portrayed that at every position of triangular bar flow diverges from its original path and flow circulation takes place over the chips, and also behind the bar in a counter clockwise direction. Furthermore much stronger circulation takes place between the chips compared to without vortex case. It's also signifies the heat transfer enhancement, which also depend upon the position of the triangular bar. So it is important to find out the optimum position of the triangular bar to get uniform heat transfer rate.

6.2. Effect of Reynolds Number

In Figure 5(a-c) temperature contour and streamline shown at different Reynolds number at a particular position of vortex. Temperature contours tells that with increasing Reynolds number thermal boundary layer separation takes place and thickness of the layer decreases with increasing Reynolds number. Flow circulation behind the triangular bar and strength of the circulation that takes place between the chips increases with increasing Reynolds number. Both signify the enhancement of heat transfer.

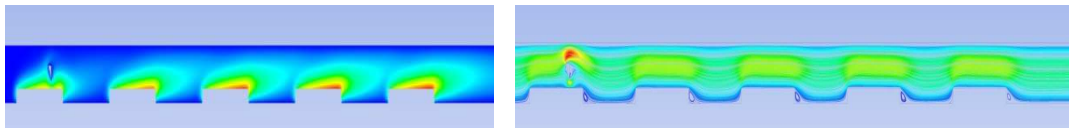


Figure 5(a): Temperature Contour & Streamline at Re= 50, Vortex Position $x/H=6.5$, $y/H=0.4$

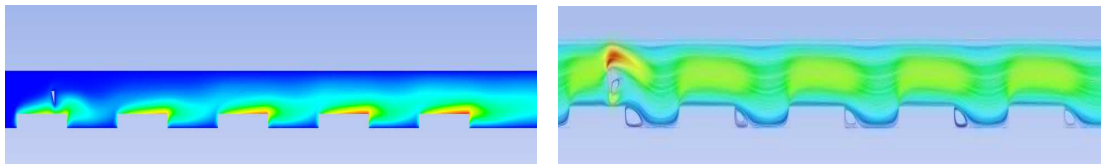


Figure 5(b): Temperature Contour & Streamline at Re= 150, Vortex Position $x/H=6.5$, $y/H=0$

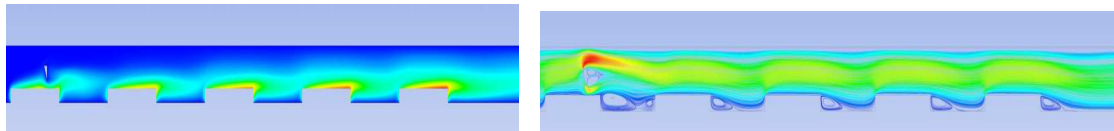


Figure 5(c): Temperature Contour & Streamline at Re= 250, Vortex Position $x/H=6.5$, $y/H=0.4$

6.3. Effects of Position of Vortex

6.3.1. Effect of x/H on Heat Transfer

It has found that due the inclusion of the triangular bar which act as a vortex generator heat transfer enhanced. Now it is important to find out the positional effects of the vortex. The effects of vortex on local Nusselts number and average Nuseelts number are shown in a graph at Figure 6-9. Variation in local Nusselts number at Chip 1 with respect to Reynolds number for different position of vortex shown. Where it is found that maximum local Nusselts number present at the vortex position $x/H=6.5$, because the triangular bar present just top of the first Chip as shown in Figure.5. Due to the bar flow circulation takes place above the first chip so maximum heat transfer takes place at that chip. Similarly in Figure. 7 shows that maximum local Nusselts number of Chip 2 present at the vortex position $x/H=8.5$ as because the triangular bar in that case present just in front of the second chip, due to this some vortices generate between first and second chip and same time flow circulation behind the bar takes place at tip of second chip. So due to the position of the triangular bar different chip have different local Nusselts number with varying Reynolds number.

In Figure 8 a graph has been plot between average Nusselts number with respect to Reynolds number at different

position of the vortex generator. All those graphs also represent that triangular bar inclusion within the channel much beneficial than the channel without vortex in terms of heat transfer enhancement. Average Nusselt number with varying the x/H , shown in Figure.9 at different Reynolds number.

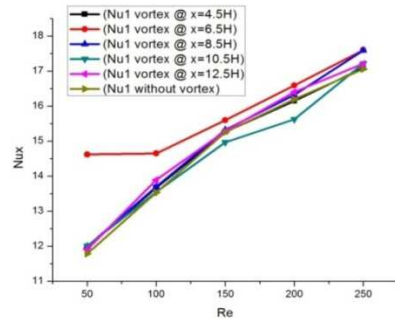


Figure.6

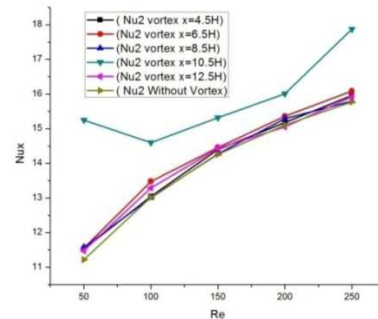


Figure 7

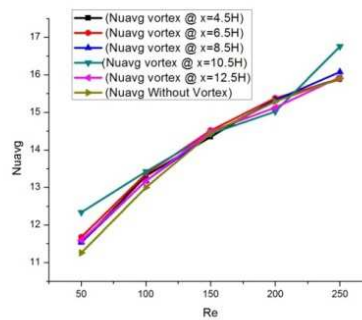
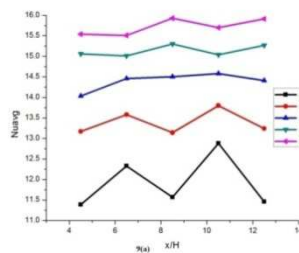
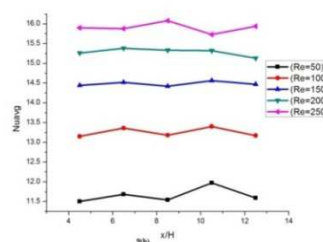
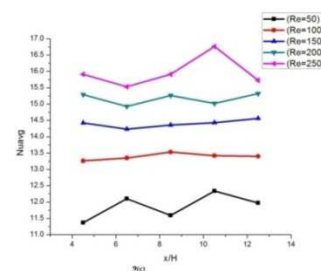


Figure 8

Figure 9: (a) at $y/H=0.3$,(b) at $y/H=0.4$ (c) at $y/H=0.35$

5.3.2 Effects of y/H on Heat Transfer

Vortex positions in Y-direction also have some effect on local Nusselt number as well as average Nusselt number within the channel. Movement of the triangular bar in positive Y-direction will increase the local heat transfer as well as average heat transfer. Probable reason could be the clearance between the chip and the bar. It will increase the velocity of the air at the top of the chip as shown in Figure. 10. In this present study based on bar position of $y/H = 0.3, 0.35$ and 0.4 . Maximum clearance present at $y/H=0.4$. So maximum heat transfer takes place at that position.

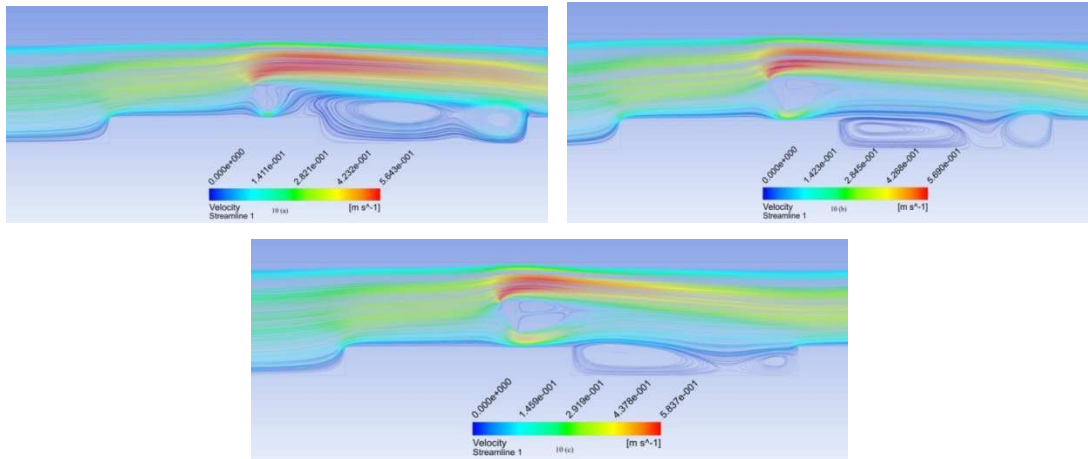


Figure 10: (a) Streamline at y/H=0.3, (b) Streamline at y/H= 0.35, (c) Streamline at y/H=0.4

5.3. Statistical Optimization for Improvement of Average Nuselts Number

Multiparameter optimization was done to show the interaction among the independent variables such as vortex position (x/H, y/H) and Reynolds number. Table no. 3 represents the design of matrix and simulation results. Theoretical model generated is given as

$$Nu_{avg} = 12.682 + 0.0363 \frac{x}{H} - 18.73 \frac{y}{H} + 0.03950 Re - 0.000266 \frac{x}{H} * \frac{y}{H} + 25.90 \left(\frac{y}{H}\right)^2 - 0.000064 Re^2 - 0.0025 \frac{x}{H} * \frac{y}{H} - 0.000125 \frac{x}{H} * Re + 0.00880 \frac{y}{H} * Re. \quad (15)$$

The regression analysis ($R^2=0.99$) indicates the concurrency of the simulation data with the model. The obtained Fischer variance ratio (F) was found to be 6.64 (significance level: $\alpha=0.05$).

Table No 3: Matrix and Result of a Three Factor Box-Behnken Design

Trial No.	Position of Vortex Along X axis (x/H)	Position of Vortex Along Y Axis (y/H)	Reynolds Number(Re.)	Average Nusselt Number (Nuavg)
1	4.5	0.3	150	14.35
2	8.5	0.3	250	15.93
3	8.5	0.4	250	16.08
4	12.5	0.35	50	11.62
5	12.5	0.35	250	15.95
6	4.5	0.4	150	14.44
7	12.5	0.4	150	14.49
8	4.5	0.35	50	11.37
9	8.5	0.35	150	14.36
10	8.5	0.35	150	14.36
11	8.5	0.35	150	14.36
12	8.5	0.3	50	11.57
13	12.5	0.3	150	14.41
14	8.5	0.4	50	11.54

15	4.5	0.35	250	15.91
----	-----	------	-----	-------

In table no.3, trial no. 3, it was observed that maximum average Nusselt number of 16.08. It could be due to the presence of a triangular bar between first and second chip. The probable reason for above observation could be due to creation of some local vortices between the two chips and flow circulation due to the bar at the tip of second chip. This could have probably improved the heat transfer in both the chips. It was also observed that with increasing Reynolds number heat transfer increases.

In Figure 10. Response surfaces shown. For the response shown in Figure 10 (a) P-value is 0.032, for Figure 10(b) P-value is 0.020 both much less than significance level $\alpha = 0.05$, that shows good mutual interaction with average Nusselt number. But in Figure. 10(c) P-value is 0.975 higher than significance level which means that mutual interaction between x/H & y/H do not taking place as changing x/H vortex position changes from one chip to another chip.

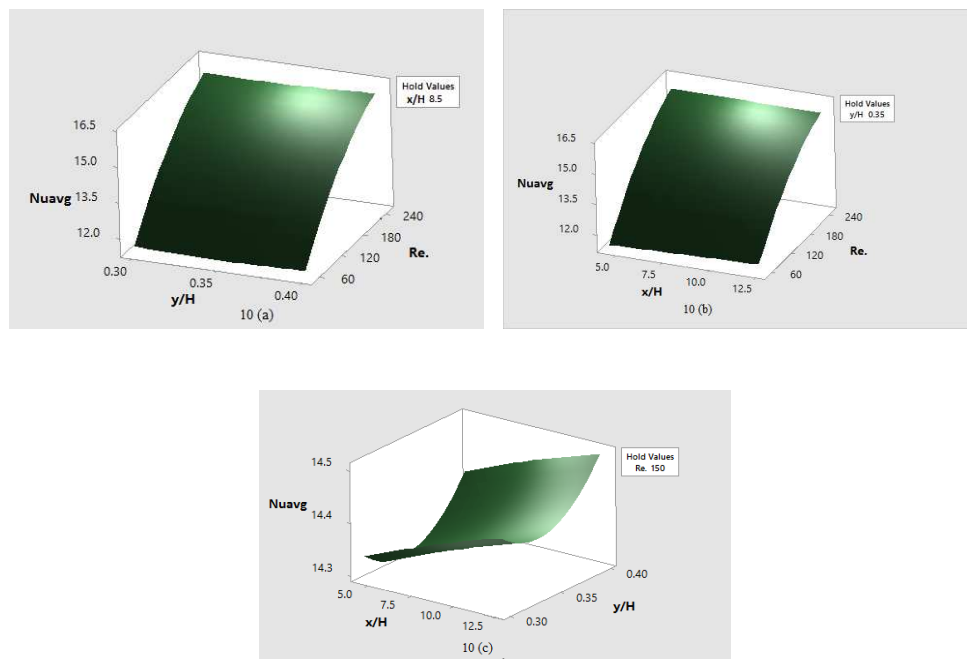


Figure 10: Response Surface Plots. (a) Nuavg vs y/H and Re. (b) Nuavg vs x/H and Re. (c) Nuavg vs x/H and y/H

In response curve Figure. 10(a) its clearly state that average Nusselts number increases with increasing Reynolds number and the position y/H , similarly in response curve Figure. 10(b) states the increment of heat transfer takes place with increasing Reynolds number and position x/H of the bar, which proves that earlier results as mention in Para 5.3.1 and 5.3.2 are right. Through regression optimum vortex position was $x/H=7.65152$ and $y/H=0.4$ and Reynolds number was $Re=250$ for the given model . After simulation using the optimum vortex position and Reynolds number, value of average Nusselt number came to be 15.92. So this model fits good for the proposed objectives.

7. CONCLUSIONS

The numerical study of laminar mixed convective heat transfer in a horizontal channel including five electronic chips mounted in bottom wall with a vortex generator (triangular bar), VG, is carried out in order to maximize heat transfer. The parameters changed are: Reynolds number ($Re= 50, 100, 150, 200$, and 250) and different location of vortex generator ($x/H= 4.5, 6.5, 8.5, 10.5, 12.5$ and $y/H= 0.3, 0.35$, and 0.4). The results of the study lead to the following

conclusions:

- Heat transfer increases with the Reynolds number due to thermal boundary layer separation and thickness of the layer decreases.
- the flow circulation behind the triangular bar and strength of the circulation that takes place between the chips also increase with the Reynolds number.
- the triangular bar inclusion within the channel much beneficial than the channel without vortex in terms of heat transfer enhancement.
- the movement of the triangular bar in positive Y-direction will increase the local heat transfer as well as average heat transfer.
- the maximum Nusselt number (average) is obtained at $x/H = 8.5$ and $y/H = 0.4$ and $Re=250$.

REFERENCES

1. M.M. Mousa, Air cooling characteristics of a uniform square modules array for electronic device heat sink, *Applied Thermal Engineering* 26 (2006) 486-493.
2. L. Graetz, Ueber die Wärmeleitfähigkeit von Flüssigkeiten, *Ann. Phys. Chem., Part 1* (18) (1883) 79-94; L. Graetz, Ueber die Wärmeleitfähigkeit von Flüssigkeiten, *Ann. Phys. Chem., Part 2* (25) (1885) 337-357
3. W. Elenbaas, Heat dissipation of parallel plates by free convection, *Physica* 9 (1) (1942) 1-28.
4. S. Ostrach, Combined natural and forced convection laminar flow and heat transfer of fluids with and without heat sources in channels with linearly varying wall temperature, *NACA TN 3141*, 1954.
5. Sugato Ghosh, Inertia Effect Under Couple Stress Fluid in Laminar Flow on Porous Journal Bearing, *International Journal of Mechanical and Production Engineering Research and Development (IJMPERD)*, Volume 5, Issue 5, September - October 2015, pp. 1-12
6. R.K. Shah, A.L. London, in: T.F. Irvine, Jr., J.P. Hartnett (Eds.), *Advances in Heat Transfer, Supplement 1, Laminar Flow Forced*
7. *Convection in Ducts: A Source Book for Compact Heat Exchanger Analytical Data*, Academic Press, New York, 1978.
8. S. Ostrach, in: F.K. Moore (Ed.), *High Speed Aerodynamics and Jet Propulsion, Laminar flows with body forces, Section F, Theory of Laminar Flows*, vol. IV, Princeton University Press, Princeton, New Jersey, 1964, pp. 528-718.
9. G.D. Raithby, K.G.T. Hollands, in: W.M. Rohsenow, J.P. Hartnett, E.N. Ganic (Eds.), *Handbook of Heat Transfer Fundamentals*,
10. *Natural Convection*, Section 6, second ed., McGraw-Hill Book Co., New York, 1985, pp. 6-1-6-94.
11. W. Aung, in: S. Kakac, R.K. Shah, W. Aung (Eds.), *Handbook of Single Phase Convective Heat Transfer, Mixed Convection in Internal Flow*, Section 15, John Wiley & Sons, New York, 1987, pp. 15-1-15-55.
12. H.W. Wu, S.W. Perng, Effect of an oblique plate on the heat transfer enhancement of mixed convection over heated blocks in a horizontal channel, *Int. J. Heat Mass Transfer* 42 (1999) 1217-1235.
13. A. Valencia, Heat transfer enhancement due to self sustained oscillating transverse vortices in channels with periodically mounted rectangular bars, *Int. J. Heat Mass Transfer* 42 (1999) 2053-2062.

14. A. Sohankar, L. Davidson, *Effect of inclined vortex generators on heat transfer enhancement in a three-dimensional channel*, *Num. Heat Transfer Part A* 39 (2001) 433–448.
15. S.J. Yang, *A numerical investigation of heat transfer enhancement for electronic devices using an oscillating vortex generator*, *Num. Heat Transfer Part A* 42 (2002) pp.269–284.
16. Q. Wang, Y. Jaluria, *Unsteady mixed convection in a horizontal channel with protruding heated blocks and a rectangular vortex promoter*, *Phys. Fluids* 14 (7) (2002) 2113–2127.
17. S. Alahyari Beig, E. Mirzakhali, F. Kowsari, *Investigation of optimal position of a vortex generator in a blocked channel for heat transfer enhancement of electronic chips*, *International Journal of Heat and Mass Transfer* 54 (2011) 4317–4324.
18. G.E.P. Box, K. Wilson, *On the experimental attainment of optimum conditions*, *J. R. Stat. Soc.* 13 (1951) 1-45.
19. Jiandong Zhou et al, *Design of microchannel heat sink with wavy channel and its time-efficient optimization with combined RSM and FVM methods*; *International Journal of Heat and Mass Transfer*; 103 (2016) pp.715–724.
20. Huai-Zhi Han, *Multi-objective shape optimization of double pipe heat exchanger with inner corrugated tube using RSM method*, *International Journal of Thermal Sciences*; 90 (2015), pp. 173-186
21. Sina Lohrasbi, *Multi-objective RSM optimization of fin assisted latent heat thermal energy storage system based on solidification process of phase change Material in presence of copper nanoparticles*; *Applied Thermal Engineering*; 118 (2017), pp.430–447
22. Box GEP, Behnken DW. *Some new three level designs for the study of quantitative variables*. *Technometrics* 1960;2:455e75.